



John, R.S. and Batchelor, A.R. and Ivanov, D and Udoudo, O.B. and Jones, D.A. and Dodds, Chris and Kingman, S.W. (2015) Understanding microwave induced sorting of porphyry copper ores. *Minerals Engineering*, 84 . pp. 77-87. ISSN 0892-6875

Access from the University of Nottingham repository:

<http://eprints.nottingham.ac.uk/30606/1/MINE-D-15-00530%20Manuscript.pdf>

Copyright and reuse:

The Nottingham ePrints service makes this work by researchers of the University of Nottingham available open access under the following conditions.

This article is made available under the Creative Commons Attribution Non-commercial No Derivatives licence and may be reused according to the conditions of the licence. For more details see: <http://creativecommons.org/licenses/by-nc-nd/2.5/>

A note on versions:

The version presented here may differ from the published version or from the version of record. If you wish to cite this item you are advised to consult the publisher's version. Please see the repository url above for details on accessing the published version and note that access may require a subscription.

For more information, please contact eprints@nottingham.ac.uk

Understanding microwave induced sorting of porphyry copper ores

R.S. John^{a*}, A.R. Batchelor^a, D. Ivanov^b, O.B. Udoudo^a, D.A. Jones^a, C. Dodds^a,
S.W. Kingman^a

^a Department of Chemical and Environmental Engineering, University of Nottingham,
University Park, Nottingham, NG7 2RD, United Kingdom

^b Royal School of Mines, Imperial College London, London, United Kingdom

* Corresponding author. Tel.: +44 (0)115 951 4080; E-mail address:
becca.john@nottingham.ac.uk (R.S John)

Abstract

Global demand for minerals and metals is increasing. It has been established that the impact of mining and mineral processing operations must be reduced to sustainably meet the demands of a low grade future. Successful incorporation of ore sorting in flow sheets has the potential to improve energy efficiency by rejecting non-economic material before grinding. Microwave heating combined with infra-red temperature measurement has been shown to distinguish low and high grade ore fragments from each other. In this work, experimentally validated 2-D finite difference models of a theoretical two phase ore, representing typical fragment textures and grades, are constructed. Microwave heating is applied at economically viable energy inputs and the resultant surface thermal profiles analysed up to 2 minutes after microwave heating. It is shown that the size and location of grains can dramatically alter surface temperature rise at short thermal measurement delay times and that the range of temperatures increases with increasing fragment grade. For the first time, it is suggested that increasing the delay time between microwave heating and thermal

measurement can reduce the variation seen for fragments of the same grade but different textures, improving overall differentiation between high and low grade fragments.

Keywords

microwave, ore, copper, sorting, modelling

1 Introduction

The mineral processing industry's current ability to meet the demands of a low grade future has prompted discussion about a required step change (Bearman, 2013). Current flow sheets are highly energy intensive; estimates suggest that comminution alone accounts for around 2% of worldwide electricity demand (Napier-Munn, 2014). With global concerns surrounding climate change, the mining industry is under pressure to improve environmental sustainability by reducing energy, greenhouse gas and water footprints (Pearce et al., 2011), whilst meeting increasing demands for minerals and metals (Fu, 2012), as ore grades are falling (USGS, 2012).

For both existing and new mineral processing operations, early rejection of gangue via sorting (at fragment sizes typically found in primary and secondary crusher products) has significant potential to reduce grinding energy. Non-economic material can be removed from the comminution process before significant energy costs are incurred through the grinding stages (Pokrajcic, 2010). Whilst a number of ore sorting technologies are available and have been demonstrated at industrially relevant scales for commodities such as diamonds (Riedel and Dehler, 2010), limestone and industrial minerals (Sivamohan and Forssberg, 1991), none have been

proven to give the required discrimination for the low grade porphyry copper ores that account for around 60% of future global copper resources (BGS, 2007).

Microwave (MW) energy has been shown to have benefits across a range of mineral processing applications including microwave assisted comminution of ores (Kingman et al., 2004, Jones et al., 2005), enhanced magnetic separation (Kingman and Rowson, 2000), leaching (Al-Harashseh and Kingman, 2004) (Al-Harashseh, 2005) and exfoliation of vermiculite (Folorunso et al., 2012). MW energy provides selective and volumetric heating; semi-conductive sulphide minerals such as pyrite and chalcopyrite have been shown to heat significantly more than rock forming minerals such as quartz and feldspar (Walkiewicz, 1988).

Low power microwave attenuation has been successfully used to sort diamond bearing kimberlite from gabbro in a process developed by De Beers (Sivamohan and Forssberg, 1991, Salter and Nordin, 1993). A 100mW 10.535 GHz microwave signal was applied to ore fragments; the level of attenuation of the signal was used to either accept or reject each fragment. The technology was successfully scaled to a 100 tonne per hour prototype by replacing the scintillation counter of an M17 radiometric sorting unit with the microwave attenuation system.

The earliest attempt to use microwave heating to discriminate between ore fragments was by Berglund and Forssberg, who investigated microwave sorting of a Zinkgruvan sulphide ore (Berglund and Forssberg, 1980). Ore fragments were heated in a multimode microwave cavity and the temperature rise of each fragment measured. No information is available on the sorting criteria, however it was stated that losses of 20% Pb and 25% Zn to the reject fraction were considered too high to warrant further investigation (Sivamohan and Forssberg, 1991).

Microwave heating combined with temperature measurement was studied in further detail by Van Weert and Kondos (2007). The exploratory study on high sulphide and carbonaceous rocks aimed to reject the highly carbonaceous fragments responsible for preg-robbing in cyanide leaching of gold. Test fragments were placed around the edge of the turntable in a 1.1kW multimode MW cavity operating at 2.45 GHz for 20s. Fragments were removed from the cavity and the maximum temperature measured using an infra-red (IR) gun, and classified as either hot, medium or cold. Sulphidic and carbonaceous fragments were concentrated in the hot class, however it was not possible to distinguish between sulphidic and carbonaceous fragments based on the maximum temperature measured. Additionally, the orientation of fragments during microwave treatment affected the measured temperature. Although the results were promising in terms of sortability, no attempt was made to quantify the microwave energy input and therefore the economic viability of the process.

A subsequent study by Van Weert et al. (2009) aimed to establish potential conditions for MW-IR sorting of a range of molybdenum and copper sulphide ores. This work established that significant upgrades in valuable mineral content were achievable using the technique. However, as the tests were not carried out in a consistent manner, with different treatment times used for each ore; microwave energy inputs were not quantified, making comparison between different samples very difficult. Furthermore, with maximum surface temperatures of over 100°C, selectively heated mineral phases are likely to have reached much higher temperatures, possibly leading to surface oxidation or even melting of sulphides. As noted in early microwave comminution work by Kingman et al. (2000), such mineral alterations can have negative impacts on downstream flotation processes, due to changes in mineral surface chemistry.

Van Weert et al. (2011) subsequently conducted a study into the microwave heating rates of a range of sulphide minerals. All minerals were crushed to produce two size fractions (approximately 2000 μm and $-74 \mu\text{m}$). The coarser size fraction was tested as both separated grains and touching (heaped). Higher heating rates were reported when grains were touching, whilst slower microwave heating rates were measured for the finer size fraction. These observations may be due to increased loss of heating to the surrounding due to increased surface area to volume ratio. The conductivity and resulting skin depth of the minerals is also likely to have influenced heating rates, however these were not considered in the investigation.

Recently, MW-IR sorting has been applied to the gradation of iron ores (Ghosh et al., 2013, Ghosh et al., 2014). 30 fragments of approximately 10mm were randomly selected from larger samples (mass unknown). Specimens were arranged in a rectangular array on the turntable of a 1.25 kW multimode cavity and heated for 10s (the time for one revolution). Fragments were then removed from the cavity and imaged using an IR-camera. Tests were repeated 5 times with the same fragment placement and results reported as repeatable, however no attempt was made to place fragments in different positions on the turntable and it was assumed that each fragment received the same cumulative microwave energy dose. In reality this is unlikely, due to the relatively small size of the fragments and the standing wave patterns inherent in domestic multimode microwave cavities.

Following Labview analysis, fragments were classified as either high grade (70% fragment surface at or above 50°C) or low grade (40% fragment surface below 50°C). Subsequent chemical assay indicated concentration of iron in the high grade class (67.3%) compared to the low grade class (54.4%). Although the sorting

correlation was good, the use of MW-IR sorting for iron ore on a fragment by fragment basis may not be economically viable, due to the relatively high grade of all fragments; again microwave energy input was not quantified.

Recently, a method has been proposed for studying the microwave heating of ores with controlled mineralogies, by using synthetic samples (Rizmanoski and Jokovic, 2015). This is achieved by embedding sulphide mineral grains within a microwave transparent gangue matrix. Previous attempts using a cement or plaster matrix were unsuccessful; larger sulphide grains settled at the bottom of synthetic ore fragments and fragments were too brittle for repeated testing (Van Weert and Kondos, 2008, Rizmanoski and Jokovic, 2015). Rizmanoski developed a fabrication method using poly methyl methacrylate (PMMA) to bind pulverised quartz, creating a hardwearing matrix with dielectric properties similar to those of quartz.

The objective of the paper is to determine the potential for microwave-infrared sorting of ores in multimode cavities with power densities in the order of $1 \times 10^8 \text{ W/m}^3$. Finite difference modelling will be used to determine the microwave heating behaviour of binary ore fragments at a quantified and economically feasible microwave energy input of 0.5 kWh/tonne of ore. Three broad textural aspects will be considered; grain location, grain dissemination and grain size. Synthetic fragments are fabricated using the method developed by Rizmanoski (2015), with textures matching those modelled. Synthetic fragments are treated in a multimode cavity at 2.45 GHz and an equivalent microwave energy dose. Comparison of the modelled and experimental surface temperature rise allows validation of the numerical models. Subsequently, a range of discrete grades representative of fragments in low grade porphyritic ores will be modelled, specifically 0%, 0.10%, 0.25%, 0.35%, 0.55%, 0.65%, 0.85%, 1.00% and

2.00% copper content. The influence of fragment texture and grade on the sorting process will be discussed with respect to potential pilot scale MW-IR ore sorting processes.

2 Materials and methods

Previous experimental work has shown that microwave heating combined with infrared thermal measurement of fragments' surfaces (MW-IR sorting) can be used to broadly differentiate between high grade and low grade ore fragments based on temperature rise (Van Weert et al., 2009) However, the effect of ore fragment texture, and the response of different textures at different fragment grades commonly seen in porphyry copper ore sorting feed stocks at economically viable microwave energy inputs have not yet been investigated.

In this paper, numerical modelling is used to determine the likely microwave heating response of binary fragments with different textures and grades, to determine the suitability of MW-IR for sorting ore feeds comprising fragments of differing textures. In this work, binary refers to an ore consisting of two minerals only. To validate these models, synthetic fragments of corresponding size, texture and similar microwave heating characteristics are heated in a microwave cavity. The thermal response of these fragments is measured and the results used to validate the representation of binary ore heating and surface thermal profile development. An additional set of binary models are used to determine the range of thermal responses exhibited by fragments of different textures, at grades commonly seen in porphyry copper ores. Finally, the conclusions drawn from the modelling results and their implications for microwave-IR sorting of ores at an industrial scale are discussed.

2.1 Numerical modelling of the microwave heating of binary ore fragments

Numerical modelling was undertaken using a 2-D finite difference geotechnical software package, FLAC Version 6.0 (ITASCA, 2008). Binary ore fragment models were constructed to investigate the heating of chalcopyrite grains within a quartz matrix. The selection was based on chalcopyrite being one of the most common copper sulphide minerals in porphyry copper ores, and quartz being one of the most common rock forming minerals (USGS, 2008). Chalcopyrite has been previously shown to be a strong microwave absorber (Cumbane, 2003), whilst quartz is effectively transparent in the microwave region (Church et al., 1988). The thermal and mechanical properties of both minerals are also well defined. Whilst a binary ore model is a drastically simplified system compared to real ore fragments, it was considered necessary to construct models in this way to assist experimental validation and to determine the effects of different textures on the surface thermal profiles of fragments. This approach has been also previously shown to be successful in modelling microwave assisted breakage of ores (Jones et al., 2005). The aim of the investigation is therefore to use FLAC (Fast Lagrangian Analysis of Continua) to model binary ore fragments with heated phase grain size and dissemination patterns akin to those found in real ore fragments.

Three textural factors will be considered, specifically grain location, grain size and grain dissemination. Simulated microwave heating will be applied to the chalcopyrite phase at power densities and treatment times similar to those in the microwave cavity used for synthetic fragment testing. A 'cooling' period will be added to represent the thermal measure delay time inherent in a proposed pilot scale sorting system, between microwave heating and thermal imaging.

The thermal imaging of modelled fragments will be approximated by measuring the temperature rise at predefined points around the binary fragments edges. The data from these thermal profiles can be used as a basis for comparison for experimental testing of the synthetic fragments.

2.1.1 Geometrical construction

The construction of the model ore was carried out by randomly disseminating grains of microwave absorbing chalcopyrite in a microwave transparent quartz matrix. The total fragment sized was fixed as a circle of 40mm diameter. This is within the range of ore fragment sizes typically found in primary and secondary crusher products that would be the target for fragment by fragment ore sorting applications.

Based on the accuracy required, the computing power available for this work and the solving time, a balance was struck for the size and number of zones. For finer chalcopyrite grains, the resolution was increased to ensure that temperature gradients around grains could be accurately captured by the model. Initial scoping studies showed no significant change in modelling results when manually placing grains (of equivalent area and in equivalent locations) in the finest and coarsest grids. To simplify the random dissemination of grains using FLAC's built in programming language, FISH (short for FLACish), it was decided to make the size of each zone the same as the size of grains to be disseminated.

Table 1: Model geometry for 40mm binary fragments

Chalcopyrite grain size μm	Grid size (zones)	Total zones
50	800x800	640000
150	268x268	71824
300	134x134	17956

Initial models were run for fragments of constant grade to allow direct comparison of thermal data. Binary ores were assigned a composition of 1% by mass of chalcopyrite (equivalent to 0.35% Cu, a typical lower threshold for ore classified as low grade) and 99% by mass of quartz. To understand the effect of mineralisation location, the position of 50 μm grains disseminated in 5% of fragment area was varied from the centre to the edge of the fragment.

To examine the effect of grain size, dissemination was kept constant, whilst grains of 50, 150 or 300 μm were randomly disseminated at 1% total content in 100% area of the modelled ore fragment. These three grain sizes were chosen to represent those typically found in copper porphyry ores.

Finally, to examine the effect of dissemination, 50 μm chalcopyrite grains were randomly disseminated in 3 fixed areas of 10, 50 and 100% of the total ore fragment.

Figure 1 represents the different textures considered in FLAC models; the red dashed regions denote the dissemination volumes of chalcopyrite grains within each quartz fragment.

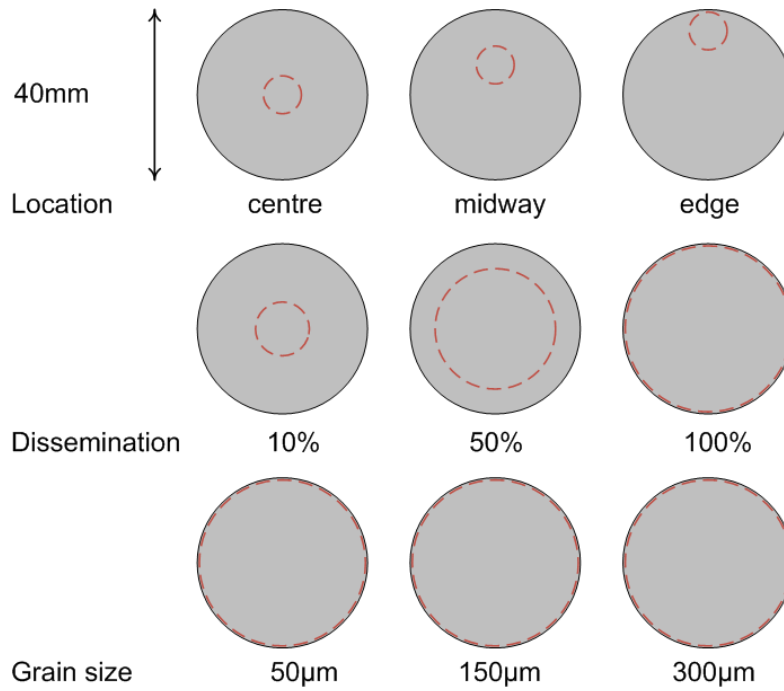


Figure 1: Chalcopyrite grain dissemination areas for simulated quartz ore fragments

2.1.2 Modelling of microwave heating

The power absorption density in a material due to dielectric heating is a function of internal electric field strength within the material, the frequency of the microwave radiation and the dielectric properties of the material. For a uniform electric field, this is given by Equation 1.

$$P_d = 2\pi f \varepsilon_0 \varepsilon'' E_o^2 \quad (1)$$

Where P_d is the power dissipation density (W/m^3); f is the frequency of the microwave radiation (Hz); ε_0 is the permittivity of free space (8.854×10^{-12} F/m); ε'' is the material's dielectric loss factor; E_o^2 is the magnitude of the electric field portion of the microwave energy within the material (V/m) (Metaxas and Meredith, 1983).

In this work it is assumed that P_d is constant in the absorbing chalcopyrite phase and zero in the transparent phase, and that chalcopyrite heats volumetrically. Quartz and other rock forming minerals are very poor absorbers of microwave energy and thus do not contribute to fragment heating. Although simplistic, previous work on modelling microwave heating of binary ores have shown these assumptions to be realistic (Jones et al., 2005, Ali and Bradshaw, 2009).

An appreciation of possible mineral skin depths is required to justify using volumetric heating within chalcopyrite grains, as opposed to modelling heating at skin depth. Table 2 gives minimum and maximum literature conductivities for a range of common ore minerals (Pridmore and Shuey, 1976, Shuey, 1975, Harvey, 1928, Telkes, 1950, Domenicali, 1950, Theodossiou, 1965, Slichter and Telkes, 1942, Sleight and Gillson, 1973, Mansfield and Salam, 1953). Corresponding skin depths are calculated according to Equation 2:

$$\delta_s = \left(\frac{2}{\sigma \omega \mu_0} \right)^{\frac{1}{2}} \quad (2)$$

Where δ_s is the skin depth (m); σ is the electrical conductivity of the material (S/m); ω is the angular frequency ($2\pi f$ rad/s); μ_0 is the permeability of free space ($4\pi \times 10^{-7}$ m.kg/C²).

The skin depth of chalcopyrite at 2.45 GHz is between 25 and 1800 μm based on literature values for conductivity (see Table 2). Given that grains will heat to skin depth around their perimeter, skin depths of 150 μm are required to heat the largest 300 μm grains studied; this is a fair assumption based on the literature range for chalcopyrite conductivity.

Table 2: Conductivities and skin depths of minerals at 2.45 GHz

Mineral		Conductivity σ S/m	Skin depth δ μm
Chalcopyrite	min	2.00E+00	1802
	max	1.00E+04	25
Pyrite	min	1.00E+00	2549
	max	1.00E+05	8
Bornite	min	3.33E+02	140
	max	5.00E+04	11
Chalcocite	min	2.38E+01	522
	max	2.00E+04	18
Magnetite	min	5.00E+03	36
	max	9.09E+03	27
Pyrrhotite	min	6.25E+03	32
	max	5.00E+05	4
Galena	min	1.72E+00	1943
	max	3.33E+05	4
Ilmenite	min	5.00E-01	3604
	max	1.00E+02	255
Cubanite	min	1.00E+00	2549
	max	1.00E+00	2549
Arsenopyrite	min	1.43E+02	213
	max	6.67E+04	10
Molybdenite	min	1.00E-06	2548749
	max	4.17E+02	125

A power density value in the chalcopyrite of $3.6 \times 10^8 \text{ W/m}^3$ was selected. This is based on previous electromagnetic modelling of a potential pilot scale microwave sorter conducted at the University of Nottingham (Dimitrakis, 2010). Two seconds of heating is applied to the chalcopyrite phase; this is equivalent to 0.5 kWh applied microwave energy per tonne of ore, which is deemed to be an economically viable microwave energy input for the pre-concentration of low grade copper ores.

2.1.3 Modelling of heat transfer

FLAC allows the transient heat conduction in materials to be simulated; the differential expression of the energy balance has the form:

$$-q_{i,i} + q_v = \rho C_p \frac{\delta T}{\delta t} \quad (3)$$

where q_{ii} is the heat flux vector which is governed by the Fourier's law (W/m^3); q_v is the volumetric heat intensity (W/m^3) which is equated to the power density inside the material; ρ is the density of the material (kg/m^3); C_p is the specific heat capacity ($J/kg.K$).

2.1.4 Material properties data

The densities of minerals were obtained from Mindat (2014), specific heat capacities at room temperature from taken from Knacke et al (1991), thermal conductivities at room temperature from Horai and Simmons (1969), thermal expansion coefficients from Clark (1966) and elastic properties from Bass (1995). It is assumed that thermal and mechanical properties of constituent minerals used are typical of those minerals. Table 3 gives the values for material properties used in the FLAC models.

Thermal properties are known to vary with temperature, however, as only relatively low temperature rise values (20-80°C) were studied in this modelling, a single value for each parameter was chosen. It is appreciated that this is a simplified approach however in reality the changes seen in the fragment thermal profiles when using slightly different thermal properties would be insignificant compared to the differences in thermal profiles of fragments with different grades. It should also be noted that typically, only single values for thermal and mechanical properties are quoted in literature for the temperatures targeted in this modelling work, further suggesting only small variations within this range.

Table 3: Thermal and mechanical properties of minerals

Property	Unit	Quartz	Chalcopyrite
Density	kg/m ³	2650	4200
Specific heat capacity	kJ/kg.K	0.74	0.54
Thermal conductivity	W/m.K	7.0	30.0
Thermal expansion coefficient	K ⁻¹	3.3x10 ⁻⁷	1.7x10 ⁻⁵
Bulk modulus	Pa	3.64x10 ¹⁰	1.40x10 ¹¹
Shear modulus	Pa	3.114x10 ¹⁰	4.47x10 ¹⁰

2.1.5 Data extraction

To monitor the surface temperature of the modelled fragments, history points were positioned every 10° around the fragment circumference. The temperature at these points was recorded (at a rate of 2 measurements per second) for the 2 seconds of applied microwave heating and for 120 seconds after, to monitor the evolution of surface temperature with time.

2.1.6 Modelling assumptions and justifications

It is assumed that the square grid used in FLAC provides a suitable approximation for the range of grain geometries found in real ores. FLAC has previously been used to successfully model microwave heating and thermal stress development in binary ores at grain sizes similar to those studied here (Jones et al., 2005, Whittles et al., 2003).

Real ores naturally contain micro scale flaws between grains whereas in FLAC models there are no discontinuities between quartz and chalcopyrite grain phases, It is assumed that this will not significantly alter the overall heating profiles compared to real fragments as discontinuities in real ores are very small compared to the overall fragment size (µm compared to cm).

Measuring modelled fragment temperature at 36 points around the circumference and then averaging can be approximated to average surface temperature for real microwave heated ore fragments. Thermal temperature measurement of real ore fragments is achieved by imaging a fragment surface and averaging the temperature measured at each pixel to give a single temperature. Thus both methods are averages of multiple point temperatures, though with different numbers of points.

3 Experimental validation of synthetic fragment modelling

3.1 Heated phase characterisation

The heated phase selected for this investigation was a copper concentrate sample originating from a North American mine. To ensure that the fraction of microwave heating minerals was correct in each synthetic fragment and for each size class, mounts were prepared for scanning electron microscope mineral liberation analysis (SEM-MLA). The copper concentrate sample was wet sieved and then dry sieved using a root 2 sieve series to give clear separation of the different size fractions. Statistically representative samples prepared from the sieved fractions of the copper concentrate were split with a small box riffle and Quantachrome Microriffler to obtain sub-samples of 1-5-2.0g. This sub-sample was cold mounted in epoxy resin and left to cure overnight. The cured samples underwent grinding and polishing using a Struers Rotapol polisher. To prevent charging of the mounts when presented to the SEM, the mounts were carbon coated applying a thin film (~30 nm) of carbon to each mount using a JEOL JEE-420 carbon coater.

For each of the size classes tested, between 1 and 6 mounts were prepared for microanalysis; these were the number of mounts required to meet the 25000 particle count required for robust results in the analysis of each size class. Mineralogical

characterisation was undertaken using the FEI Quanta 600i SEM. The mineralogical and textural information was extracted using the MLA version 3 software designed by FEI Company (FEI, 2013) The measurement mode of the software was the 'Extended backscatter' (XBSE) mode, which segments minerals based on their backscatter (greyscale) differences. Subsequently an X-ray is collected on a centroid spot on each different mineral phase delineated by the greyscale differences. The X-ray spectra profile is used to identify the mineral phase using the EDAX Genesis 4000 energy dispersive (EDS) software. The EDS classification involves matching collected spectra to a spectra database. The surface area of the various classified particles is computed to generate the weight % composition of minerals. The results of this analysis are presented in Figure 2.

SEM-MLA analysis indicated that the copper concentrate was composed predominantly of chalcopyrite (50-65 wt%), and also included notable quantities of pyrite, bornite and molybdenite. A number of other microwave susceptible metal sulphide and oxide minerals (chalcocite, galena, enargite and ilmenite) were also present in minor quantities. The copper concentrate also contained minor amounts of non-heating rock forming minerals, such as quartz, biotite and muscovite. The overall quantities of chalcopyrite (the principal heated phase) reduce with increasing size class; this is expected as the number of fully liberating grains will be higher at small grain sizes' whilst larger grains may still be attached to small amounts of gangue.

Overall, the total proportion of microwave heating sulphide and oxide minerals versus non-heating rock forming minerals was at least 80% in each size class. Masses of concentrate for each synthetic fragment fabricated were scaled to ensure the same

fraction of heating minerals in each size class used. It was assumed that each heating mineral within the concentrate would exhibit similar heating rates at 2.45 GHz, as indicated previously by the dielectric properties of minerals measured by Genn (2013) and would thus provide a suitable representation for the chalcopyrite used in the FLAC models with respect to individual grain heating and thermal profile development.

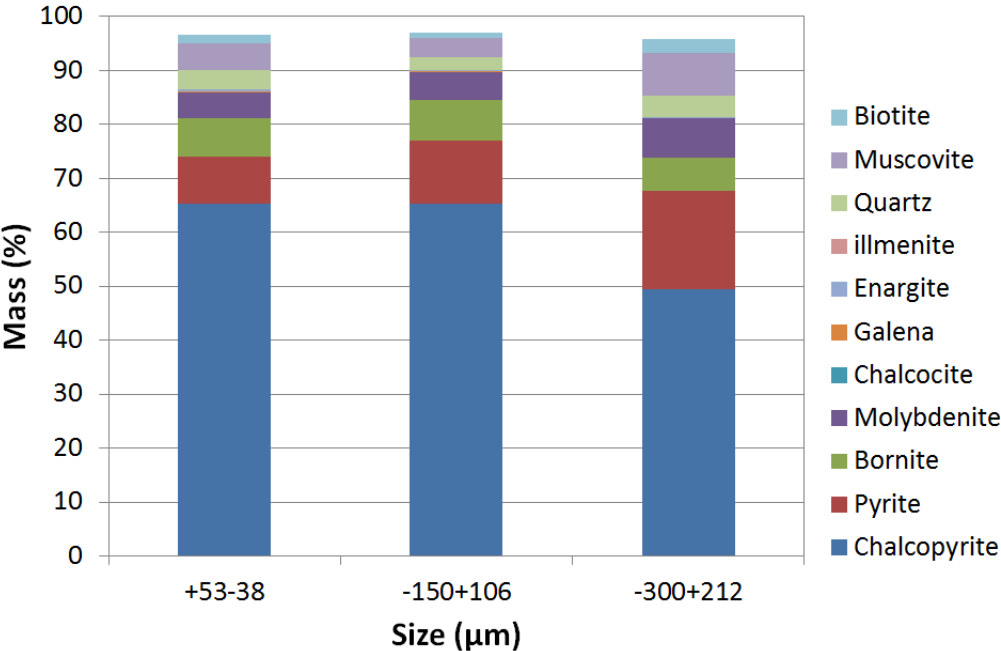


Figure 2: Copper concentrate major mineralogy by size class

3.2 Synthetic fragment fabrication

The method used to fabricate the matrix for synthetic fragments is covered in detail elsewhere (Rizmanoski and Jokovic, 2015). The synthetic fragments were fabricated in 40mm half-sphere silicon moulds to provide samples of the same size used in FLAC modelling and to remove any heating effects due to fragment geometry. The ‘transparent gangue’ matrix was created from pulverised quartz sand and bound together with Lecoset 100, a polymethyl methacrylate (PMMA) 2-part powder/liquid

mix, commonly used for making mounts for microanalysis (LECO, 2014). Lecoset binder was chosen to give thermal and mechanical properties similar to that of real ores (when used as a binder for quartz/silica) and also for its low dielectric loss, so it would not contribute to microwave heating.

3.3 Microwave heating testing methodology

Fragments were tested individually in a 3.3kW multimode cavity at 2.45 GHz, equipped with a mode stirrer. Incident microwave power was set to 1.1kW and fragments were placed in the centre of the cavity on the turntable. Microwave power was applied for 12s, the time for one revolution. As each fragment had the same mass and was placed in the same position within the microwave applicator, it was assumed that they were all exposed to the same amount of microwave energy. In reality, the different textures could lead to slightly different mode patterns within the applicator, meaning that microwave treatments could be subtly different. However by using a multimode applicator significantly large in size than the fragments, together with the mode stirrer, any differences in microwave treatment were minimised.

After microwave heating, each fragment was then removed and placed under an NEC H2640 640x480 pixel resolution thermal imaging camera for 60s to provide comparative thermal data to FLAC models. In FLAC, thermal data was averaged for all history points around the 2D model circumference. To get comparative thermal images, fragments were heated and imaged in four different orientations. Average and maximum temperature rise values were averaged for each orientation and also for duplicate texture fragment. Thermal images were recorded and analysed via Radiometric Complete Online, a commercial program suitable for the online and offline analysis of thermal images (Radiometric Infrared Solutions, 2011). Thermal

images were analysed to extract the maximum and average temperature for each fragment tested, before and after treatment. Average temperature rise was used as the basis of comparison with FLAC data as maximum temperature rise only corresponds to the hottest pixel measured.

4 Results and Discussion

4.1 Numerical modelling results

4.1.1 Effect of grain location on fragment surface thermal profiles

Fragments were modelled with 1% 50 µm chalcopyrite grains disseminated in 5% of total ore volume (see Figure 1). Figure 3 shows the average and maximum temperature rise values for the three different mineralisation locations, after a 60s thermal measurement delay time (2s heating, 58s cooling). Figure 3 indicates that the average surface temperature rise after 60s varied from 2.2 to 3.8°C according to mineralisation. As expected, the highest average and maximum temperatures occurred for the fragment with mineralisation closest to the surface, with the centralised mineralisation giving the smallest temperature rise. For this fragment there is little difference between average and maximum temperatures as the length of the thermal conduction path from the centre to edge of the fragment is virtually identical.

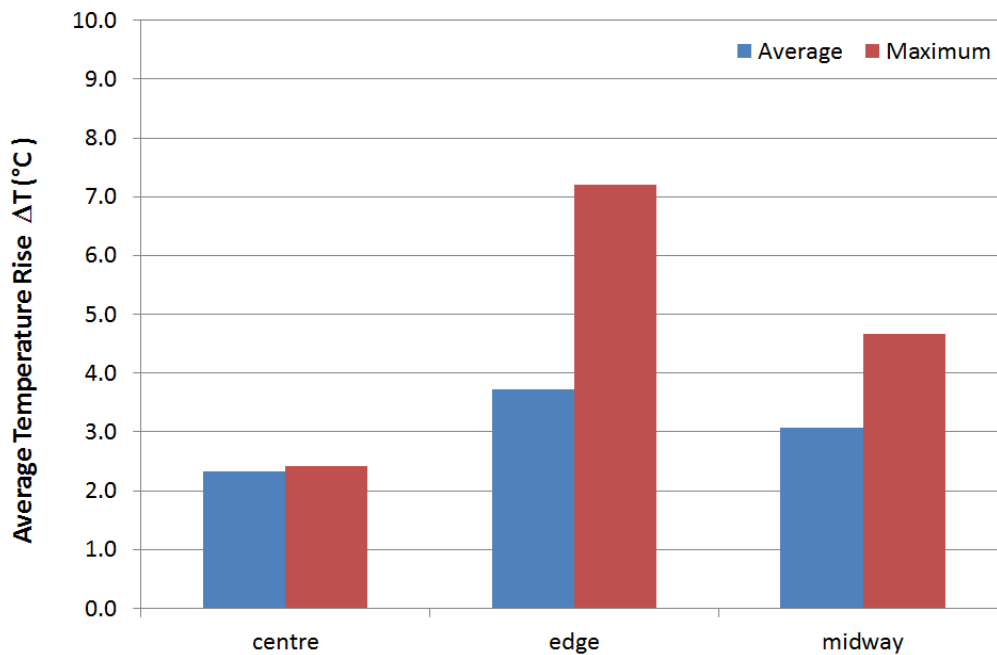


Figure 3: Average and maximum temperature rise around modelled fragment circumference, 1% 50 μm chalcopyrite, varied location, 60 second delay time

To determine how temperature rise for the different textures varies with time, Figure 4 plots the temperature recorded at each data history point for each of the three mineralisation locations over a 120s period (2s heating, 118s cooling). There are clear differences in the range of surface temperatures after 120s cooling, however the lower temperature for each fragment is very similar, around 22°C. It should be noted that the peak surface temperature for each fragment occurs at significantly different times, around 8 seconds for the edge mineralisation, 20s for midway and 40s for the centralised grains.

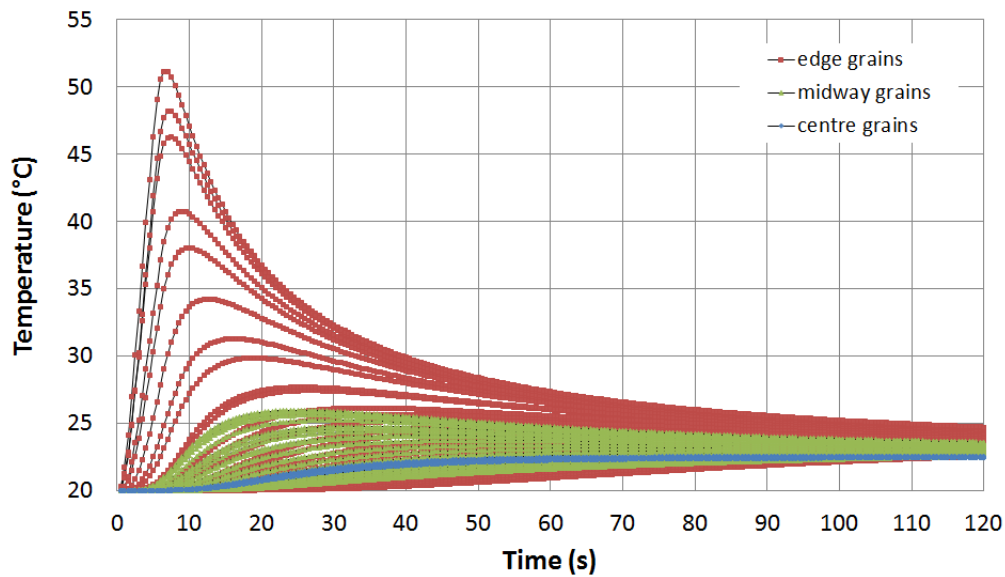


Figure 4 Surface Heating and Cooling Profile for 1% 50 µm chalcopyrite with varying mineralisation grain location

4.1.2 Effect of dissemination on fragment surface thermal profiles

Fragments were modelled with 1% 50 µm chalcopyrite grains disseminated in 10, 50 and 100% of the ore fragment volume (see Figure 1). Figure 5 shows the average and maximum temperature rise values for the three dissemination levels at 60s thermal measurement delay time. The lowest temperature rise values are for the 10% and 100% fragments, with average temperature rise values of 2.3 and 2.8°C respectively. The 100 % dissemination level exhibits significantly higher average and maximum temperature rise values; these are likely to be heavily influence by certain heated grains being closer to the surface than others. For the 10% case, the rate of heat conduction to the fragment surfaces leads to low overall temperature rise. For the 50% case, although some chalcopyrite grains are nearer the fragment surface,

they are more widely spread and thus heat is radiated to the surroundings (air) more rapidly.

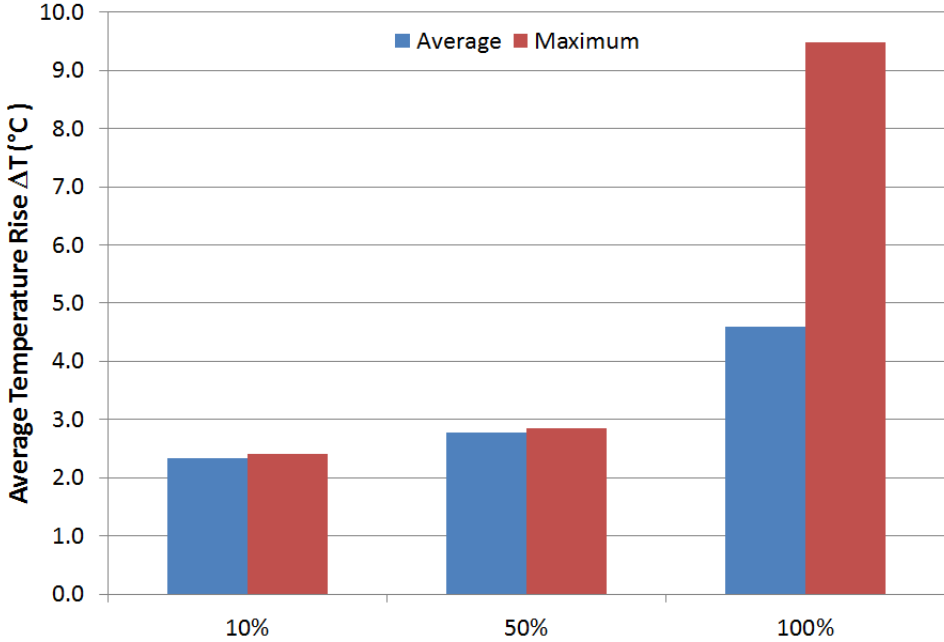


Figure 5 Average and maximum temperature rise around modelled fragment circumference, 1% 50 μm chalcopyrite, variable dissemination, 60 second delay time

Figure 6 plots the temperature at each data history point over 120s. For the 100% dissemination case, a sharp spike in temperature can be seen for one of the history points; this indicates proximity to a heated grain or possibly a small cluster caused by the random dissemination code utilised.

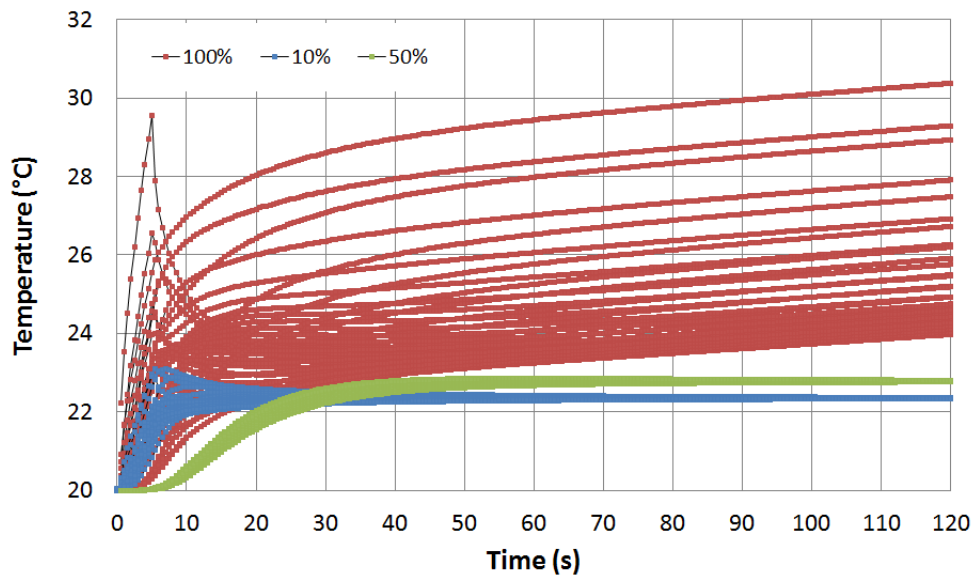


Figure 6 Surface Heating and Cooling Profile for 1% 50 µm chalcopyrite with varying dissemination levels

There are differences in the delay time to maximum measured surface temperature; however by 30s the 10 and 50% dissemination models show similar thermal profiles. The 100% case exhibits very different behaviour in the range of surface temperatures measured, even after 2 minutes. To better understand these differences, Figures 7 to 10 present thermal images of the 100% dissemination model exported from FLAC during modelling at 1,5,10 and 30s delay times. Areas of the same colour in each image represent areas of the fragment within the same temperature band. The initial image at 1s delay time (during microwave heating) highlights the random but uneven distribution of chalcopyrite grains with the entire fragment volume, including a number of grains at or close to the fragment surface, which cause a peak in fragment surface temperature at 5 seconds. As heat is conducted from high to low (grid) zones, a complex heating pattern develops which eventually progresses to a banded thermal profile with the upper right quadrant of the fragment hottest. This accounts

for the large range of temperatures recorded at each history point around the fragment surface.

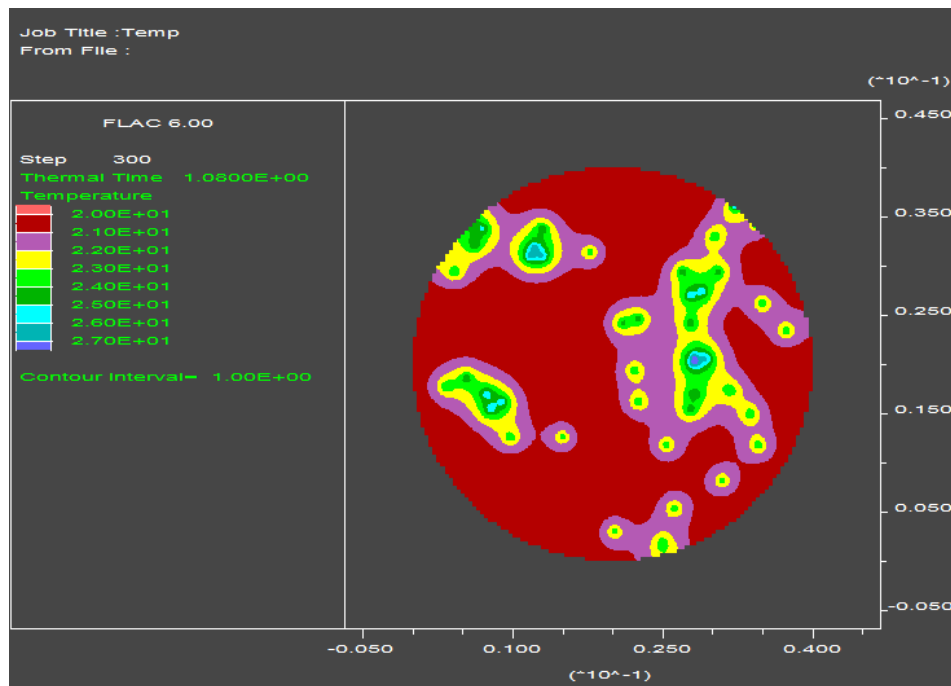


Figure 7 Thermal profile evolution, 1% 50 μm chalcopyrite, 100% dissemination, 1s delay time, temperature $^{\circ}\text{C}$

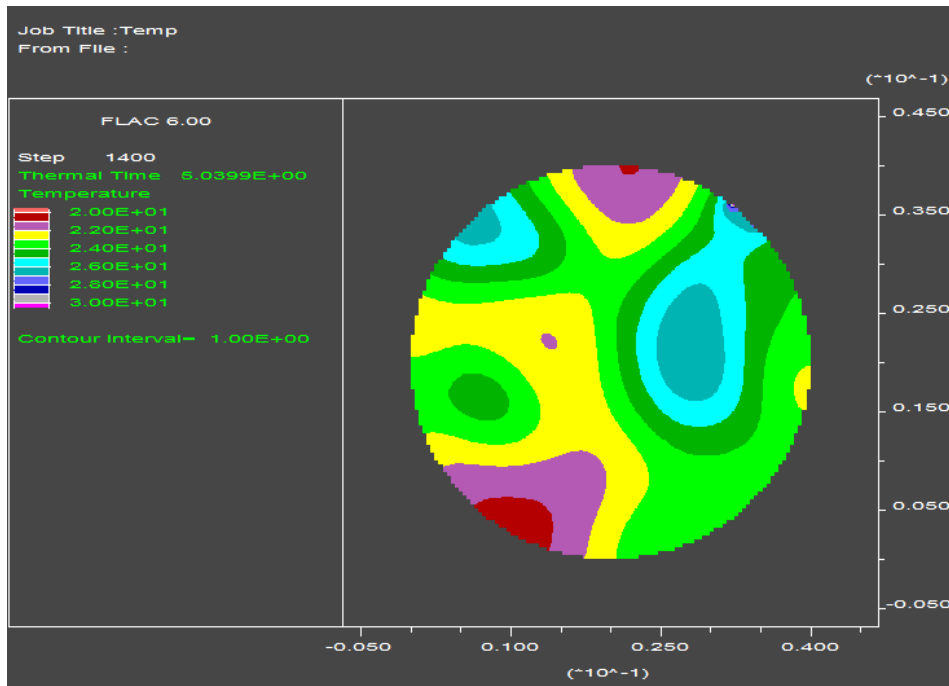


Figure 8 Thermal profile evolution, 1% 50 μm chalcopyrite, 100% dissemination, 5s delay time, temperature $^{\circ}\text{C}$

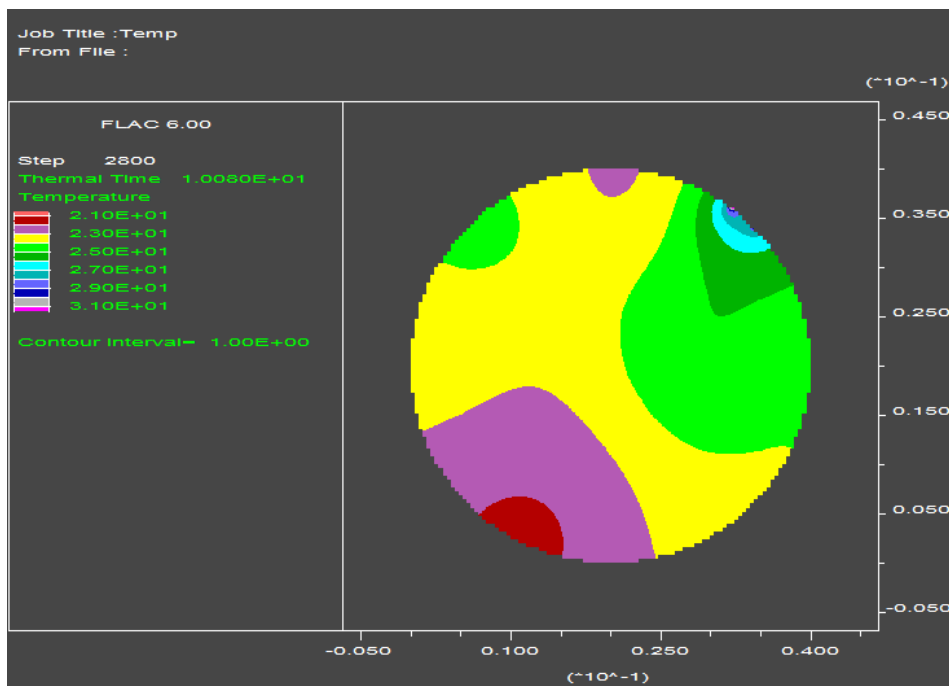


Figure 9 Thermal profile evolution, 1% 50 μm chalcopyrite, 100% dissemination, 10s delay time, temperature $^{\circ}\text{C}$

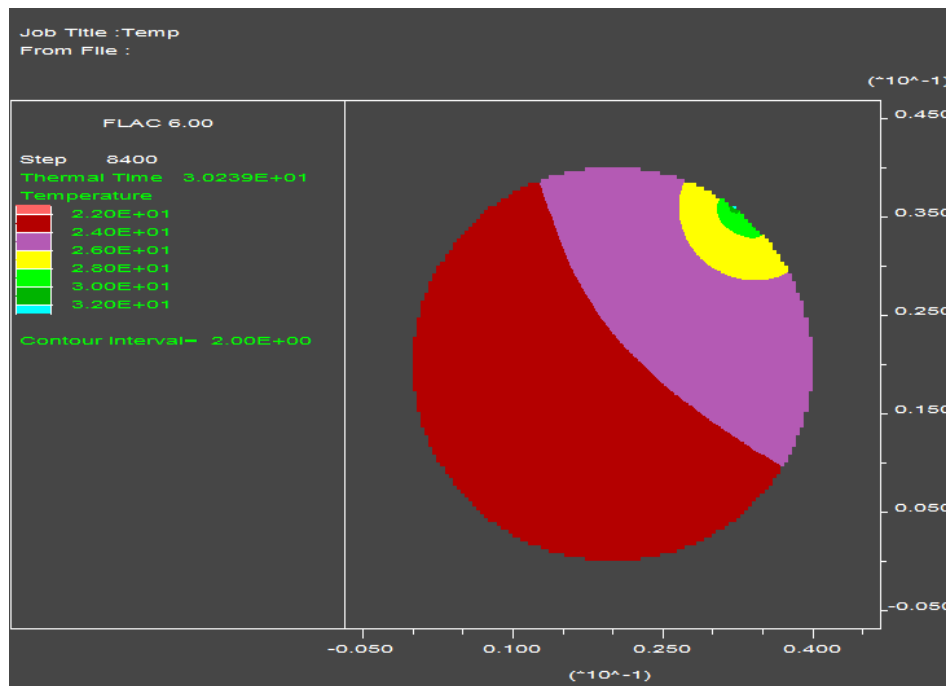


Figure 10 Thermal profile evolution, 1% 50 μm chalcopyrite, 100% dissemination, 30s delay time, temperature $^{\circ}\text{C}$

4.1.3 Effect of grain size on fragment surface thermal profiles

Fragments were modelled with 1% chalcopyrite grains disseminated in 100% of the total ore fragment volume (see Figure 1). Chalcopyrite grains modelled were 50, 150 and 300 μm . Figure 11 shows the average and maximum temperature rise values for the three different grain sizes, after a 60s thermal measurement delay time. Figure 3 indicates that the average surface temperature rise after 60s varied from 2.2 to 3.8 $^{\circ}\text{C}$ according to mineralisation. Average and maximum temperature rise increases with decreasing grain size, with the 50 μm grains showing the highest temperature rise. This is due to the increased surface area available for conduction of heat into the quartz matrix. At longer thermal measurement delay times (2 minutes) the average temperature for the different grain size fragments was almost identical.

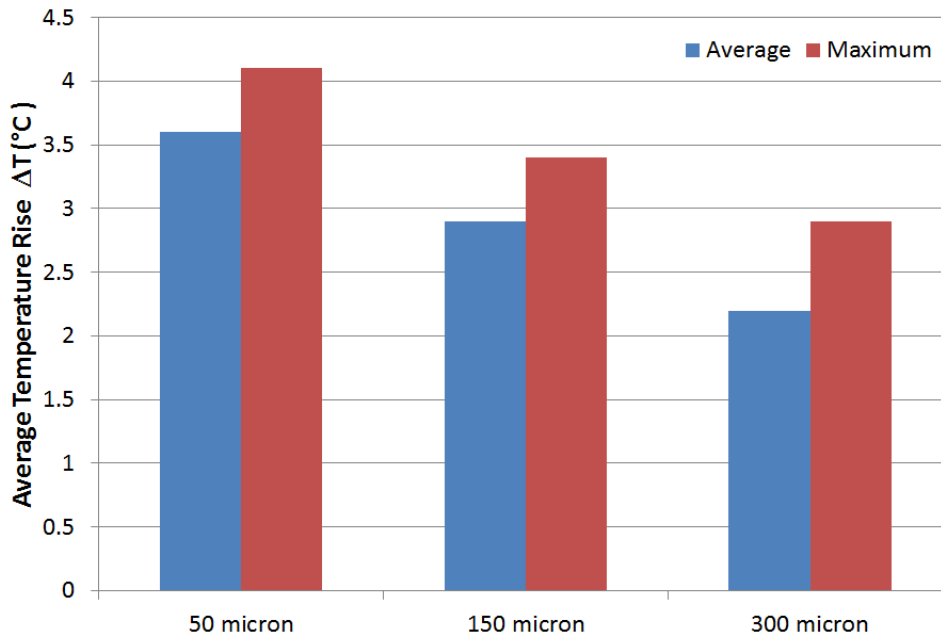


Figure 11 Average and maximum temperature rise around modelled fragment circumference, 1% chalcopyrite, 50/150/300 μm , 100% dissemination, 60 second delay time

4.2 *Experimental validation of modelling*

Figure 12 presents a direct comparison of FLAC and microwave test results on synthetic fragments at a 60s measurement delay time. Generally there is good agreement between modelled and the microwave heated fragments, with the exception of the 100% dissemination case where significant clustering of grains in the FLAC model led to increased average surface temperatures, as previously shown in figures 7 to 10. Overall, the temperature rise values are lower in the synthetic fragments than in the FLAC models, although some heating (0.3°C) was observed in the blank synthetic fragment.

Temperature was measured at fixed history points around the circumference of the FLAC fragments and then averaged. Thermal images of synthetic fragments were averages of the entire surface presented to the IR-camera, in four different fragment orientations.

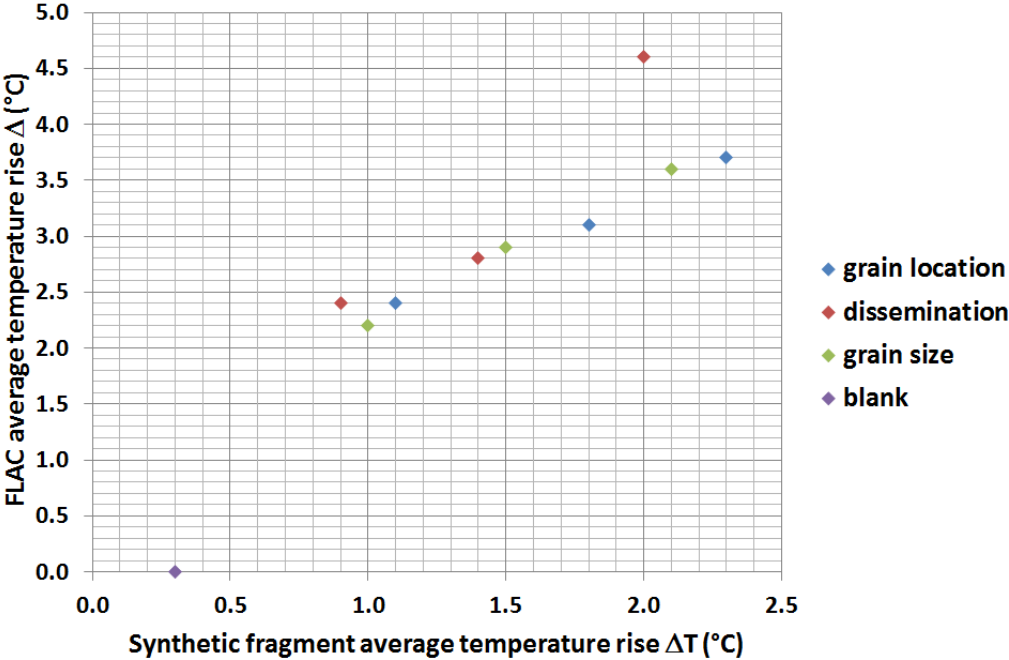


Figure 12 Comparison of FLAC and synthetic fragment average temperature rise, 60s delay time

The differences between FLAC model and synthetic fragment results may be attributed to a number of factors. In FLAC, fragments are modelled in two dimensions (as an infinite cylinder) whilst synthetic fragments produced were three dimensional spheres. This will lead to some differences in thermal conduction; however as both cases are based on radial conduction and surface temperature measurement the overall trends are comparable.

The 0.3°C temperature rise in the barren synthetic fragment also point to differences between simulated and real microwave heating. Whilst it was assumed that the

power density in the gangue phase was zero for FLAC modelling, it is clear that some power was absorbed in the gangue. This would in turn lead to a different power density in the heated phase. The gangue phase comprised a quartz PMMA mix; whilst this was chosen to have similar thermal and dielectric properties to pure quartz, any differences in these properties could lead to changes in thermal profiles.

The position of heated grains was also different in synthetic fragments compared to FLAC; whilst equivalent dissemination volumes were used for both cases, within these volume grains were positioned randomly.

FLAC models consisted of chalcopyrite grains of a single size. Obtaining copper concentrate grains of a single size was not feasible for the fabrication of synthetic fragments, so single size classes were used. Variability in grain size in synthetic fragments is likely to have caused minor differences in the rate of heat transfer from heated grains to the gangue matrix, as demonstrated by the increasing maximum and average surface temperature rise values for the smallest grain sizes in both FLAC and synthetic fragments.

It is also assumed that 100% of power is absorbed in the FLAC model, whereas in multimode experimental treatments power absorption is likely to have been lower. Finally, any discontinuities in contact between copper concentrate grains and the gangue matrix would reduce the rate of heat transfer; this was not incorporated into the FLAC models.

Differences between FLAC and synthetic fragments results suggest that whilst there is good correlation between the trends for binary fragments, further development of the model is required to provide a robust tool that accurately predicts the average thermal profiles of fragments of different textures.

4.3 Variation of fragment average temperature rise with copper grade

Additional FLAC models were run, representing the same three texture variations modelled previously, but at a wider range of chalcopyrite (copper) contents. These were chosen to cover the range of grades typically seen in fragments of the size suitable for fragment by fragment sorting. The precise copper grades selected reflect assumed cut-off grades for different ore designations. For each model, surface temperatures were recorded at 18 history points around the fragment circumference rather than the previous 36 to reduce computation time and the quantity of data produced. Although this reduced the detail of thermal data, the average temperature rise could still be calculated with reasonable accuracy. Models were run to 60s (2 seconds heating plus 58 seconds cooling); the frequency of thermal data acquisition was also reduced to once per second as the additional points were not required for comparison between different fragment grades.

Figure 13 shows the average temperature rise for modelled fragments after 60s. As fragment grade increases, the variation in thermal profiles for different textures increases. At two percent copper content, individual fragment temperature rise ranges from 4.5 to 12°C. This increase in spread is due to the increase in the number of grains; the more grains in a fragment, the greater the potential clustering of grains, leading to a wider range of fragment thermal profiles.

There is slight deviation in the trends for each individual texture type; specifically the order of fragments (of the same grade but different texture) from hottest to coldest changes between different grades. This is due to the random dissemination of grains in a portion of each of the models. Grain location within the dissemination areas could not be kept consistent due to the differing number of grains in each modelled

fragment. As such any 'bias' in grain distribution would lead to increased temperature rise on one of two areas of the fragment, thus deviating the overall trend for that texture type. Edge grains located directly on the surface of fragments rather than just below can lose heat more rapidly early in the 'cooling' process. By 60 seconds the average surface temperature can be less than that of a centre grained texture, as in the centre and edge grain fragments modelled at 0.85% copper.

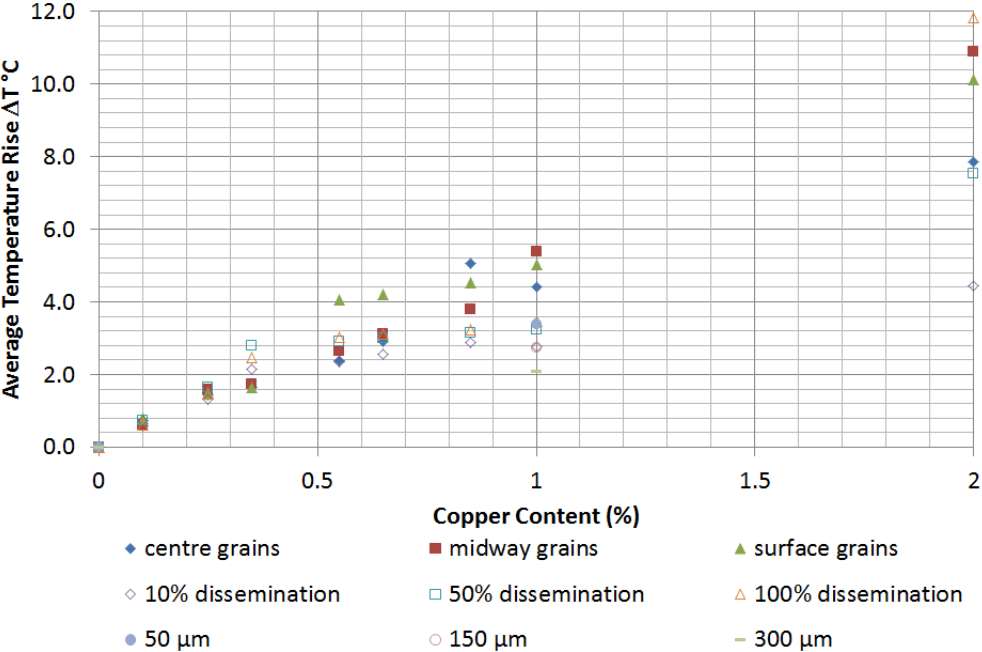


Figure 13 Average temperature rise at 60s measurement delay time for FLAC modelled binary quartz and chalcopyrite ore fragments

Variables not included in this study could lead to more complex thermal profiles than those studied here. The modelled fragments were two dimensional and circular; more complex 3D geometries could lead to increased temperature rise differentials, particularly where mineralisation is located at or near the surface. This is likely in real ore fragments as the crushing and screening process to produce feeds (with a

fragment size distribution suitable for sorting on a fragment by fragment basis) often results in breakage along existing fractures, exposing mineralisation on the surface.

In assessing the implications of these results on an EM-IR sorting process, it should be reiterated that the purpose of ore sorting is not to gain a linear correlation between temperature rise and copper content, but to identify fragments that are economically barren. In Figure 13, at 0.10% copper content, no fragments have temperatures greater than (or equal to) any fragments of higher copper content. This is of course a simplified case in which only a heated valuable phase (entirely within the gangue) and a transparent matrix are present. Furthermore, the copper contents modelled are discrete values; it is likely that had fragments with copper content between 0.10 and 0.25% been modelled in FLAC, some could have temperature rise values similar to fragments at 0.10%, making textural variation more significant at lower copper content than perhaps this data shows. Industrially, this would mean optimising cut-off temperatures to either reject all lower grade fragments or accept all higher grade fragments, depending on the particular mine site.

5 Conclusions

FLAC modelling has been shown to be a useful tool for predicting trends in thermal profiles in fragments of binary mineralogy, having been experimentally validated via multimode microwave treatment of synthetic particles of corresponding texture. The following conclusions can be drawn that have implications for microwave-IR ore sorting processes:

- The size of microwave susceptible grains can affect the surface temperature rise, particularly at short thermal measurement delay times ~10 seconds. Smaller grain sizes at identical mass percentages result in a higher

temperature rise at short delay times due to the increased surface area for heat transfer.

- The location of mineralisation can be significant at short measurement delay times, with surfaces near heated grains having a higher average temperature rise. This effect was seen in both simulation and synthetic fragments where mineralisation was in one location, and also to a lesser degree when randomly disseminated grains were clustered. This is an important consideration for a belt based IR sorting system, where only one fragment orientation is imaged.
- Thermal measurement delay time has been shown to be important in thermal profiling of binary fragments; increasing the time reduces the difference in average surface temperature of fragments of different textures but with identical grade. At 10 seconds, 1% chalcopyrite fragments with grains in either centre, edge or midway locations had temperature differentials of around 25°C. At 60 and 120 seconds, this differential was reduced to 7°C and 4°C respectively.
- As the grade of fragments increases, so does variation in thermal profiles. For upgrade sorting processes applied to low/marginal grade ores, variation in high grade fragment temperature rise values should not be detrimental to recovery; providing that a suitable temperature threshold is set for accepting/rejecting fragments, all valuable fragments will still be classified as hot.
- At a fragment grade of 0.35% Cu, the temperature differential is ~1°C for the textures modelled. Assuming that variability in conditioned feed temperature

before the sorting process of $\sim 1^\circ\text{C}$ is achievable, texture can be seen as non-critical in the differentiation process below this grade.

This work has not investigated whether variations in texture and changing mineral associations have an impact on the actual electromagnetic heating of ores. Future development of FLAC ore fragment heating models could include additional mineral phases (gangue and sulphide minerals), more complex textures, angular geometries akin to those of real ore fragments, heating in the gangue phases, skin depth heating in sulphide minerals and non-perfect contact between different mineral phases.

Overall this work suggests that for copper ores of simple mineralogy, microwave-IR sorting at economically viable microwave energy inputs is indeed viable, providing that suitable systems can be designed for microwave power application, electromagnetic safety and compliance and materials handling, and that pre-sorter feed conditioning and post microwave IR imaging at suitable delay times can be achieved.

Acknowledgements

The authors would like to thank Rio Tinto Technology & Innovation for funding this work and providing mineral concentrate samples for testing.

References

- AL-HARAHSEH, M. 2005. *A fundamental investigation into the microwave assisted leaching of sulphide minerals*. PhD, University of Nottingham.
- AL-HARAHSEH, M. & KINGMAN, S. 2004. Microwave-assisted leaching—a review. *Hydrometallurgy*, 73, 189-203.
- ALI, A. Y. & BRADSHAW, S. M. 2009. Quantifying damage around grain boundaries in microwave treated ores. *Chemical Engineering and Processing: Process Intensification*, 48, 1566-1573.
- BASS, J. D. 1995. Elasticity of minerals, glasses, and melts. *Mineral Physics & Crystallography: A Handbook of Physical Constants*, 45-63.

- BEARMAN, R. A. 2013. Step change in the context of comminution. *Minerals Engineering*, 43–44, 2-11.
- BERGLUND, G. & FORSSBERG, E. 1980. Seletiv uppvärmning med mikrovagor. *Minfo Rapport nr. 0703*. Sweden.
- BGS 2007. Copper Profile. *Mineral Profiles*. Minerals UK.
- CHURCH, R. H., WEBB, W. E. & SALSMAN, J. B. 1988. Dielectric properties of low-loss minerals. *Bureau of Mines Report of Investigations RI*. US.
- CLARK, S. P. 1966. *Handbook of physical constants*, Geological society of America.
- CUMBANE, A. 2003. *Microwave Treatment of Minerals and Ores*. PhD, University of Nottingham.
- DIMITRAKIS, G. 2010. Microwave Applicator Validation. University of Nottingham.
- DOMENICALI, C. 1950. Magnetic and electric properties of natural and synthetic single crystals of magnetite. *Physical Review*, 78, 458.
- FEI 2013. MLA Software Suite. Hillsboro.
- FOLORUNSO, O., DODDS, C., DIMITRAKIS, G. & KINGMAN, S. 2012. Continuous energy efficient exfoliation of vermiculite through microwave heating. *International Journal of Mineral Processing*, 114–117, 69-79.
- FU, X. 2012. Long-term copper dynamic *International Copper Study Group (ISCG) 39th regular meeting*.
- GENN, G. L. 2013. *Novel Techniques in Ore Characterisation and Sorting*. PhD, University of Queensland.
- GHOSH, A., NAYAK, B., DAS, T. & PALIT SAGAR, S. 2013. A non-invasive technique for sorting of alumina-rich iron ores. *Minerals Engineering*, 45, 55-58.
- GHOSH, A., SHARMA, A., NAYAK, B. & SAGAR, S. P. 2014. Infrared thermography: An approach for iron ore gradation. *Minerals Engineering*.
- HARVEY, R. D. 1928. Electrical conductivity and polished mineral surfaces. *Economic Geology*, 23, 778-803.
- HORAI, K.-I. & SIMMONS, G. 1969. Thermal conductivity of rock-forming minerals. *Earth and Planetary Science Letters*, 6, 359-368.
- ITASCA 2008. 6.0: User manual. Licence.
- JONES, D., KINGMAN, S., WHITTLES, D. & LOWNDES, I. S. 2005. Understanding microwave assisted breakage. *Minerals Engineering*, 18, 659-669.
- KINGMAN, S., JACKSON, K., BRADSHAW, S., ROWSON, N. & GREENWOOD, R. 2004. An investigation into the influence of microwave treatment on mineral ore comminution. *Powder Technology*, 146, 176-184.
- KINGMAN, S. & ROWSON, N. 2000. The effect of microwave radiation on the magnetic properties of minerals. *The Journal of microwave power and electromagnetic energy: a publication of the International Microwave Power Institute*, 35, 144.
- KINGMAN, S., VORSTER, W. & ROWSON, N. 2000. The effect of microwave radiation on the processing of Palabora copper ore. *Journal of the South African Institute of Mining and Metallurgy(South Africa)*, 100, 197-204.
- KNACKE, O., KUBASCHEWSKI, O. & HESSELMAN, K. 1991. Thermochemical properties of inorganic substances. *Berlin, Heidelberg and New York, Springer Verlag*.
- LECO 2014. Met Supplies Catalogue.
- MANSFIELD, R. & SALAM, S. 1953. Electrical properties of molybdenite. *Proceedings of the Physical Society. Section B*, 66, 377.
- METAXAS, A. A. & MEREDITH, R. J. 1983. *Industrial microwave heating*.

- MINDAT. 2014. *Quartz and Chalcopyrite Mineral Densities* [Online]. Available: <http://www.mindat.org/min-955.html> , <http://www.mindat.org/min-3337.html>
 [Accessed 17/05/2014.]
- NAPIER-MUNN, T. 2014. Is progress in energy-efficient comminution doomed? *Minerals Engineering*.
- PEARCE, T. D., FORD, J. D., PRNO, J., DUERDEN, F., PITTMAN, J., BEAUMIER, M., BERRANG-FORD, L. & SMIT, B. 2011. Climate change and mining in Canada. *Mitigation and Adaptation Strategies for Global Change*, 16, 347-368.
- POKRAJCIC, Z. 2010. *A Methodology for the Design of Energy Efficient Comminution Circuits*. The University of Queensland.
- PRIDMORE, D. & SHUEY, R. 1976. The electrical resistivity of galena, pyrite, and chalcopyrite. *American Mineralogist*, 61, 248-259.
- RADIOMETRIC INFRARED SOLUTIONS 2011. Radiometric Complete 5.1 Manual
- RIEDEL, F. & DEHLER, M. 2010. Recovery of unliberated diamonds by X-ray transmission sorting. *Diamonds-Source to Use 2010*. The South African Institute of Mining and Metallurgy.
- RIZMANOSKI, V. & JOKOVIC, V. 2015. Synthetic Ore Samples to Test Microwave/RF Applicators and Processes. *Journal of Materials Processing Technology*.
- SALTER, J. D. & NORDIN, L. 1993. *Sorting method and apparatus*.
- SHUEY, R. T. 1975. *Semi-Conducting Ore Minerals*, Elsevier Scientific Publishing Company.
- SIVAMOHAN, R. & FORSSBERG, E. 1991. Electronic sorting and other preconcentration methods. *Minerals Engineering*, 4, 797-814.
- SLEIGHT, A. & GILLSON, J. 1973. Electrical resistivity of cubanite. *Journal of Solid State Chemistry*, 8, 29-30.
- SLICHTER, L. B. & TELKES, M. 1942. Electrical Properties of Rocks and Minerals. *Geological Society of America Special Papers*, 36, 299-320.
- TELKES, M. 1950. Thermoelectric power and electrical resistivity of minerals. *Am Mineral*, 35, 536-555.
- THEODOSSIOU, A. 1965. Measurements of the Hall Effect and Resistivity in Pyrrhotite. *Physical Review*, 137, A1321.
- USGS 2008. Preliminary Model of Porphyry Copper Deposits. U.S. Geological Survey.
- USGS 2012. Copper Statistics 1900-2011. In: SURVEY, U. S. G. (ed.).
- VAN WEERT, G. & KONDOS, P. 2007. Infrared recognition of high sulphide and carbonaceous rocks after microwave heating. BARRICK Gold Corporation.
- VAN WEERT, G. & KONDOS, P. 2008. Effects of susceptor size and concentration on the efficiency of microwave/infrared (MW/IR) sorting.
- VAN WEERT, G., KONDOS, P. & GLUCK, E. 2009. Upgrading Molybdenite Ores between Mine and Mill Using Microwave/Infrared (MW/IR) Sorting Technology. *41st Annual Meeting of the Canadian Mineral Processors*.
- VAN WEERT, G., KONDOS, P. & WANG, O. 2011. Microwave heating of sulphide minerals as a function of their size and spatial distribution. *CIM Journal*, 2.
- WALKIEWICZ, J. W. K., G. ; MCGILL, S. L. 1988. *Microwave heating characteristics of selected minerals and compounds*.
- WHITTLES, D., KINGMAN, S. & REDDISH, D. 2003. Application of numerical modelling for prediction of the influence of power density on microwave-assisted breakage. *International Journal of Mineral Processing*, 68, 71-91.